Beam and Channel Tracking for 5G Communication Systems Using Adaptive Filtering Techniques: A Comparison Study

Mohanad Al-Ibadi, *Member, IEEE,* and Farhad E. Mahmood, *Member, IEEE*

***Abstract*—In this paper, we study the problem of beam tracking of a multipath channel in millimeter-wave massive MIMO communication system using adaptive filters. We focus on the performance of least-mean-square filter (LMS) and recursive least-squares filter (RLS) algorithms, compared to a reference extended Kalman filter (EKF), in scenarios where the wireless channel is dominated by a single line of sight (LOS) path or a small number of strong paths. The signal direction and channel coefficients are tracked and updated using these filters. Our results recommend that beamforming systems at millimeter-wave bands should consider variable number of paths rather than a single dominant LOS path. Furthermore, we show that the mean squared-error (MSE) of the innovation process gives a better overall view of the tracking performance than the MSE of the state parameters.**

***Index Terms*—Beam tracking, Channel tracking, mmWave, multipath, LMS, RLS, EKF.**

I. Introduction

Millimeter-wave (mmWave) wireless communication systems are gaining a great amount of attention, recently, on the academic and industrial levels due to the huge available non-utilized bandwidth, in addition to the promising high data transmission rates, in the mmWave frequency bands [1]. However, these advantages come at a price, where new techniques need to be developed to deal with the signal attenuation at high-frequency transmission. As the transmission wavelength is too small at mmWave bands, the physical size of the antenna array system is small too, and a massive number of antenna elements is required to produce directional beams pointing at specific directions (e.g. user location) [2]–[4]. The effects of beam pointing errors and their impact on the performance of mmWave wireless communications system have been discussed thoroughly in the literature [5]–[7].

Narrow beamwidth at mmWave bands is an attractive feature for three main reasons: *First*, in multiuser downlink scenario, the 3 dB beamwidth is very narrow that the interference between simultaneously served users is very low, which increases the users' signal-to-interference-plus-noise ratio (SINR). *Second*, narrow beamwidth makes the communication link more immune to potential intruders, thereby raising the security of the communicating parties. *Third*, since large concentrated power is available in narrow beams (high signal-to-noise ratio, SNR), the quality of the communications link improves. However, narrow beams are sensitive to small changes in the position of the user, which necessitates the use of fast and accurate adaptive beam tracking techniques to maintain an acceptable link quality.

The beam tracking problem mainly involves the process of adaptively estimating the angular beam parameters, which are the direction of arrival (DOA) of the received signal and the direction of departure (DOD) of the transmitted signal. These two parameters represent the *state* of the tracking problem, and they need to be updated every time new data snapshots become available. The main motivation behind the need for tracking the direction of the transmitted and received signals is the relationship between the user-beam alignment and the quality of the received signal (e.g. SNR), which could be severely dropped if the user is more than 3dB away from the main beam direction [8]. Even though wide beams are more tolerant to user mobility than narrow beams, the latter guarantee better link quality, and thereby higher data transmission rates. It is worth noting that the channel coefficients between the transmitter and receiver sides need to be tracked as well in mobility scenarios. Thus, it is useful to claim channel and beam tracking when the channel coefficients, DOD, and DOA are tracked in wireless communications systems.

Different types of methods have been proposed in the literature to handle the beam tracking problem, which can be classified into two main categories. The first category is model-based, where a dynamics model is assumed to update the target state adaptively. The Kalman filter (KF) [9], [10] and the least-mean-square (LMS) algorithm [11] are among the widely used trackers under this category, where these two algorithms were used to track the DOA, DOD, and the channel gain in a mmWave wireless communication system setup. It is worth noting that the authors of these articles have concluded that the mean squared-error (MSE) of the state parameters increases over time (i.e. the KF and LMS have divergence problem in the beam-tracking application). In this letter, we show that it is recommended to inspect the MSE of the innovation process, which gives a better overall idea about the behaviour

Manuscript received October 1, 2021; revised November 2, 2021. Date of publication August 22, 2022. Date of current version August 22, 2022. The associate editor prof. Giovanni Giambene has been coordinating the review of this manuscript and approved it for publication.

M. Al-Ibadi is with the Technical College of Engineering/Najaf, at Al-Furat Al-Awsat Technical University, Najaf, Iraq (e-mail: mohanad.alibadi@atu.edu.iq).

F. E. Mahmood is with the Department of Electrical Engineering, The University of Mosul, Mosul, Iraq (e-mail: farhad.m@uomosul.edu.iq).

Digital Object Identifier (DOI): 10.24138/jcomss-2021-0117

of the trackers that are shown to have similar performance.The MSE of the state parameters represents the average of the squared error between the measured DOA and DOD and their estimated values over time. On the other hand, the MSE of the innovation process represents the average of the squared error between the measured and estimated observations, where there exists a mathematical model that relates the state parameters to the measured observations. Thus, the performance of the tracker is not only a function of the type of the tracker used for online estimation of the state, but also a function of the quality of the observation, as well as the mathematical model that is supposed to capture the actual physical reality to some extent.

The KF has also been used in [12], [13] to track the slow variations in the DOA and DOD angles and detect abrupt channel changes. In [14], an adaptive multistage algorithm with low feedback overhead has been proposed to track the beam and estimate the channel of a mmWave vehicular communication link. Also, the authors proposed an updated version of the extended Kalman filter (EKF) that is suitable for beam tracking in high mobility scenario. In addition, the particle filter (PF) is used to perform a beam tracking recently in the literature, such as [12], [15], [16], where, generally, the angular position of the user is described by a probability distribution that is tracked by the PF. One common advantage shared among the trackers in this category is that these algorithms are well studied and explored in the literature, and they have a predictable performance. On the other hand, they still have a few limitations, such as the linear model and Gaussian noise assumptions in the KF, and the relatively high processing time of the PF, even though they have fast convergence speeds.

The second category of beam trackers is based on machine learning algorithms (i.e. data driven approaches), such as recurrent neural networks (RNN) based on long short term memory (LSTM) architecture [17], [18], Deep SORT algorithm [19], and deep reinforcement learning [20]. These trackers are still being studied and explored in the literature to better understand their performance in different types of scenarios. Even though they have shown a promising results, the availability of training data can hinder the application of these algorithms in some situations, such as high mobility vehicles.

Our contribution can be summarized as follows:

- In this work, we investigate the recursive least-squares (RLS) algorithm as a beam tracker at mmWave bands, and compare its performance against the least-mean-square (LMS) algorithm and the extended Kalman filter (EKF) algorithm in a single path and multipath scenarios.
- We emphasise the effect of multiple paths on the performance of the tracking algorithms, where assuming a single LOS path in the presence of multiple paths can degrade the performance of the trackers. An important application to this point is the indirect paths reflected off an intelligent reconfigurable surface (IRS) [21].
- We show that looking at the average performance of the tested trackers in terms of the MSE of the innovation process is more valuable than the MSE of the state parameters, which is used in several publications in the literature, such as[9] and [11].

The paper is organized as follows. The mmWave channel model and the state-space model are presented in II. LMS and RLS algorithms are detailed in III. Our numerical results are given in IV, before we conclude our work in V.

Notation

In this paper, we use small case letters for scalars, while bold small case letters are used to denote vectors, which are assumed to be column-wise. Matrices are denoted by bold capital letters.

II. System Model

We consider a mmWave MIMO wireless communications system, where the receiver is equipped with M_R receive antennas receiving L signals originating from a transmitter equipped with M_T transmit antennas. L can be a direct path ($L = 1$) or multipath signals ($L \geq 1$), even though the number of dominant paths is usually small in mmWave channels [22]. It is worth noting that the number of paths can change over time for various reasons as the user changes its location, which can be modeled in different ways, such as a discrete-time Markov process with L states.

A narrowband geometric channel model is assumed in this work, where the steering vectors in the direction of the transmitted and received signals represent the main building component of the mathematical model [23]. In the following two sub-sections we elaborate on the theoretical background of the channel model and the beamforming model of the considered communication system.

A. mmWave Channel Model

We write the narrowband time-varying channel model for mmWave communications system at time instant k as follows [23]:

$$\boldsymbol{H}_k = \sum_{l=1}^{L_k} \alpha_{k,l} \boldsymbol{a}_{\mathrm{R}}(\theta_{k,l}) \boldsymbol{a}_{\mathrm{T}}^{\mathrm{H}}(\phi_{k,l}), \tag{1}$$

where $(\cdot)^{\mathrm{H}}$ denotes the conjugate transpose operator. L_k is the number of signal paths at time k. $\alpha_{k,l}$, $\theta_{k,l}$, and $\phi_{k,l}$ are the complex path gain, the direction of arrival (DOA), and the direction of departure (DOD) of the l-th path at time instant k, respectively. $\boldsymbol{a}_{\mathrm{R}}(\cdot)$ is the receive array response vector in the direction of $\boldsymbol{\theta}_k$ and $\boldsymbol{a}_{\mathrm{T}}(\cdot)$ is the transmit array response vector in the direction of $\boldsymbol{\phi}_k$. Generally, the array steering vectors are defined as follow:

$$\boldsymbol{a}_{\mathrm{R}}(\theta_{k,l}) = \frac{1}{\sqrt{M_R}} \left[e^{-j\Phi_1(\theta_{k,l})}, e^{-j\Phi_2(\theta_{k,l})}, \ldots, e^{-j\Phi_{M_R}(\theta_{k,l})}\right]^{\mathrm{H}}, \tag{2}$$

$$\boldsymbol{a}_{\mathrm{T}}(\phi_{k,l}) = \frac{1}{\sqrt{M_T}} \left[e^{-j\Phi_1(\phi_{k,l})}, e^{-j\Phi_2(\phi_{k,l})}, \ldots, e^{-j\Phi_{M_T}(\phi_{k,l})}\right]^{\mathrm{H}} \tag{3}$$

For a perfect linear array along the y-axis, $\Phi_i(\theta_{k,l}) = 2\pi \frac{d_i}{\lambda} \sin(\theta_{k,l})$ and $\Phi_i(\phi_{k,l}) = 2\pi \frac{d_i}{\lambda} \sin(\phi_{k,l})$, where λ is the

carrier wavelength, and d_i is the inter-element spacing of the array antennas, $i = 1, \ldots, M$.

Note that the definition of the steering vectors here can be easily extended to incorporate the elevation angle in the case of 2D arrays or a linear array in 2D space, but we restrict the discussion here to linear arrays (1D) for simplicity.

Transmit precoding and receive combining are commonly used techniques in 5G MIMO communication systems for several desirable reasons, such as a) reducing the number of RF chains (one beam per RF chain rather than one RF chain per antenna element), b) beam alignment and tracking, and c) equivalent scalar channels rather than vector channels in the conventional MIMO systems. The transmitted signal is precoded with a precoding vector, $\boldsymbol{w}_{\mathrm{T}}(\bar{\phi})$, and the received signal is combined with a combining vector, $\boldsymbol{w}_{\mathrm{R}}(\bar{\theta})$. $\bar{\theta}$ and $\bar{\phi}$ are, respectively, a pre-defined arrival and departure pointing angles. These two beamforming vectors are steering vectors in the direction of known pointing angles. Thus, $\boldsymbol{w}_R(\bar{\theta})$ and $\boldsymbol{w}_T(\bar{\phi})$ have the same mathematical form as in equations (2) and (3), respectively.

The combining and beamforming vectors are updated each time the angular distance between the pointing direction and the estimated direction of the user exceeds a specific threshold (e.g., exceeds the 3dB beamwidth). In addition, the combining and beamforming vectors should be re-estimated if the tracked path is lost, due to blockage for example [9]. In this work, we assume that there is always a LOS path between the transmitter and receiver (i.e., no blockage) over a block of time slots (100 time instances in our simulations).

The downlink received signal can now be written as follows:

$$y_k = \boldsymbol{w}_{\mathrm{R}}^H \boldsymbol{H}_k \boldsymbol{w}_{\mathrm{T}} s_k + \boldsymbol{w}_R^H \boldsymbol{n}_k, \tag{4}$$

where, s_k is a complex transmitted symbol (scalar), and $\boldsymbol{n}_k$ is a complex additive Gaussian noise with zero mean and covariance $\boldsymbol{R}_n$, that is $\boldsymbol{n} \sim \mathbf{CN}(\mathbf{0}, \boldsymbol{R}_n)$. As it is clear from equation (4), the transmit and receive pointing vectors are pre-defined and fixed and the tracker's job is to adaptively estimate the beam and channel parameters with the hope that the estimated beamforming vectors are aligned (usually up to 3dB) with the pointing vectors to achieve the best possible performance in terms of capacity, transmission power, mean squared error, or any other relevant criteria.

B. State-Space Model

In this paper, the time evolution of the DOA, DOD, and the real and imaginary parts of the complex path gain represent the "state" vector, $\boldsymbol{x}_k$, which evolves over time (the update dimension) as follows:

$$\boldsymbol{x}_k = \left[\mathbb{R}(\alpha_k), \mathbb{I}(\alpha_k), \theta_k, \phi_k\right]^T, \tag{5}$$

where $\mathbb{R}(.)$ and $\mathbb{I}(.)$ are the real and imaginary parts of a complex number, respectively. Next, we describe the state-space equations used in our work.

1) *The dynamics model*: Since we are assuming a slowly time-varying channel, it is reasonably accurate to model the state at time $k+1$ as a noisy version of the state at time k, up to a scaling factor (i.e. a random walk process). This can be written mathematically as follows [9], [11], [24], [25]:

$$\boldsymbol{x}_{k+1} = \boldsymbol{F}_k \boldsymbol{x}_k + \boldsymbol{v}_k, \tag{6}$$

where $\boldsymbol{v}_k$ is the dynamics model noise, and it captures the mismatch between the actual behaviour of the state and our understanding (and model) of this behaviour. $\boldsymbol{v}$ can be modeled as a Gaussian noise with zero mean and $\boldsymbol{R}_v$ covariance: $\boldsymbol{v} \sim N(\mathbf{0}, \boldsymbol{R}_v)$. The scaling matrix, $\boldsymbol{F}_k$, is a real square diagonal matrix, and, generally, can be modeled as follows:

$$\boldsymbol{F}_k = \mathrm{diag}\{\mathbb{R}(\rho_{\alpha_k}), \mathbb{I}(\rho_{\alpha_k}), \rho_{\theta_k}, \rho_{\phi_k}\} \tag{7}$$

ρ is a parameter that captures the correlation between two consecutive states. In this work, we impose the assumption that the angular position of the user changes slowly and smoothly. Thus, we can set $\rho_{\theta_k} = \rho_{\phi_k} = 1$, even though close-to-one values can also be used here, and we fix the values of $\mathbb{R}(\rho_{\alpha_k})$ and $\mathbb{I}(\rho_{\alpha_k})$ for all k. The elements of the matrix $\boldsymbol{F}_k$ can be measured using training data or guessed based on an educated guess. Moreover, since the elements of the matrix $\boldsymbol{F}_k$ are usually slowly time-varying, they can be efficiently tracked using simple tracking algorithm or learned in a smarter way using, for example, a machine learning type of algorithms.

2) *The measurements model*: The measurements model was given in equation (4), which can be re-written more compactly as follows:

$$y_k = h(\boldsymbol{x}_k) s_k + n_k, \tag{8}$$

where, $h(\boldsymbol{x}_k)$ is the time-varying channel impulse response (scalar and complex-valued), and, from equations (1) and (4), is given as follows:

$$h(\boldsymbol{x}_k) = \sum_{l=1}^{L_k} \alpha_{k,l} g(\theta_{k,l}) g(\phi_{k,l}). \tag{9}$$

The function $g(.)$ is defined as follows:

$$\begin{aligned} g(\theta_{k,l}) &= \boldsymbol{w}_{\mathrm{R}}^H(\bar{\theta}_l) \mathbf{a}_{\mathrm{R}}(\theta_{k,l}) = \frac{1}{M_R} \sum_{i=1}^{M_R} e^{-j\left(\Phi_i(\theta_{k,l}) - \Phi_i(\bar{\theta}_l)\right)} \\ g(\phi_{k,l}) &= \mathbf{a}_{\mathrm{T}}^{\mathrm{H}}(\phi_{k,l}) \boldsymbol{w}_{\mathrm{T}}(\bar{\phi}_l) = \frac{1}{M_T} \sum_{i=1}^{M_T} e^{+j\left(\Phi_i(\phi_{k,l}) - \Phi_i(\bar{\phi}_l)\right)}. \end{aligned} \tag{10}$$

$n_k = \boldsymbol{w}_R^H \boldsymbol{n}_k$ is a scalar measurements noise with zero mean and σ_n^2 variance: $n_k \sim \mathbf{CN}(0, \sigma_{n_k}^2)$. Note that if the actual signal direction is perfectly aligned with the pointing beam, $g(\theta) = 1$ and $g(\phi) = 1$, and the highest estimation quality can be achieved (highest SNR). As the deviation between the actual and the pointing angles increases, the received signal quality degrades and, consequently, the estimated states will be erroneous. This is a challenging problem if one or both of the communicating sides are mobile, especially in

high mobility scenarios. Thus, in real world applications, the angle deviation must be carefully monitored if a recursive algorithm is used to track and estimate the state vector to avoid unrealistic results.

Since the tracked state variables in (5) are naturally real-valued, we stack the real and imaginary parts of y_k and $h(\boldsymbol{x}_k)$ before we feed them into the tracking algorithm as follows:

$$\boldsymbol{y}_k = \begin{bmatrix} \mathbb{R}(y_k) \\ \mathbb{I}(y_k) \end{bmatrix}, \quad \boldsymbol{h}(\boldsymbol{x}_k) = \begin{bmatrix} \mathbb{R}(h(\boldsymbol{x}_k)) \\ \mathbb{I}(h(\boldsymbol{x}_k)) \end{bmatrix}. \tag{11}$$

III. Beam Tracking Algorithms

In this section, we investigate three powerful tracking algorithms to track the channel parameters (beam direction and channel gain), which were given in the state vector $\boldsymbol{x}_k$.

A. The Least-Mean-Square (LMS) Algorithm

LMS is a stochastic gradient descent-based adaptive filtering algorithm that is known for its stability and fast convergence [26]. In LMS, the state-update equation is defined as follows:

$$\hat{\boldsymbol{x}}_{k+1} = \hat{\boldsymbol{x}}_k - \boldsymbol{\mu}\boldsymbol{\nabla}_{\boldsymbol{x}_k} J_k, \tag{12}$$

where $\hat{\boldsymbol{x}}_k$ is the estimated state of $\boldsymbol{x}_k$, $\boldsymbol{\nabla}_{\boldsymbol{x}_k} J_k$ is the gradient of the mean squared-error (MSE) vector J_k, and $\boldsymbol{\mu}$ is the step size of the LMS algorithm. $\boldsymbol{\mu}$ is a diagonal matrix: $\boldsymbol{\mu} = \text{diag}\{\mathbb{R}(\mu_\alpha \mathbf{1}_L), \mathbb{I}(\mu_\alpha \mathbf{1}_L), \mu_\theta \mathbf{1}_L, \mu_\phi \mathbf{1}_L\}$, where μ_α, μ_θ, and μ_ϕ represent the values of the step size of channel path gain, DOA, and DOD, respectively. $\mathbf{1}_L$ is an all-ones vector of length L.

Assuming that the transmitted symbol has a unit norm (i.e. $\|s_k\| = 1, \quad \forall k = 1, 2, \ldots$), the error variable can be defined as the difference between the actual measurements and the estimated measurements in the following way: $e_k = y_k - h(\hat{\boldsymbol{x}}_k)$. The MSE of the innovation process can be expressed as: $J_k = \mathbb{E}\{\|\boldsymbol{e}_k\|^2\}$, where $\mathbb{E}$ is the expectation operator and, here, it is taken with respect to the probability distribution of the error vector. Furthermore, $\boldsymbol{e}_k = [\mathbb{R}(e_k), \quad \mathbb{I}(e_k)]^T$, where $\mathbb{R}(e_k)$ and $\mathbb{I}(e_k)$ are the real and imaginary parts of the estimation error. J_k contains a collective information about the variance of the measurements and the channel, in addition to the correlation between them.

By definition, the gradient of the MSE is [11], [27]:

$$\begin{aligned} \boldsymbol{\nabla}_{\boldsymbol{x}_k} J_k &= \frac{\partial}{\partial \hat{\boldsymbol{x}}_k} \mathbb{E}\{\|\boldsymbol{e}_k\|^2\}, \\ &= -2\mathbb{E}\Big\{ \boldsymbol{e}_k^T \frac{\partial \boldsymbol{h}(\hat{\boldsymbol{x}}_k)}{\partial \hat{\boldsymbol{x}}_k} \Big\}. \end{aligned} \tag{13}$$

In LMS, we are interested in the instantaneous gradient of the MSE as opposed to the average gradient in (13), which makes the LMS algorithm a good candidate for tracking non-stationary random processes. Mathematically, the stochastic gradient of J_k is defined as follows:

$$\boldsymbol{\nabla}_{\boldsymbol{x}_k} J_k = -2\boldsymbol{e}_k^T \frac{\partial \boldsymbol{h}(\hat{\boldsymbol{x}}_k)}{\partial \hat{\boldsymbol{x}}_k}, \tag{14}$$

where,

$$\frac{\partial \boldsymbol{h}(\hat{\boldsymbol{x}}_k)}{\partial \hat{\boldsymbol{x}}_k} \& = \begin{bmatrix} \frac{\partial \mathbb{R}(h(\hat{x}_k))}{\partial \mathbb{R}(\alpha_k)}, \frac{\partial \mathbb{R}(h(\hat{x}_k))}{\partial \mathbb{I}(\alpha_k)}, \frac{\partial \mathbb{R}(h(\hat{x}_k))}{\partial \theta_k}, \frac{\partial \mathbb{R}(h(\hat{x}_k))}{\partial \phi_k} \\ \frac{\partial \mathbb{I}(h(\hat{x}_k))}{\partial \mathbb{R}(\alpha_k)}, \frac{\partial \mathbb{I}(h(\hat{x}_k))}{\partial \mathbb{I}(\alpha_k)}, \frac{\partial \mathbb{I}(h(\hat{x}_k))}{\partial \theta_k}, \frac{\partial \mathbb{I}(h(\hat{x}_k))}{\partial \phi_k} \end{bmatrix} \tag{15}$$

The expression in (15) is the partial derivative of the expression in (9), which is the product of three separate terms. This makes the partial derivatives straightforward, and thus we omitted the derivation here. In addition, $\boldsymbol{h}(\boldsymbol{x}_k)$ is a two-elements vector and is derived with respect to four parameters, which makes its Jacobian matrix a $2 \times 4L$ matrix.

Accordingly, using (12) and (14), the state-update equation of the LMS algorithm is given as follows:

$$\hat{\boldsymbol{x}}_{k+1} = \hat{\boldsymbol{x}}_k + 2\boldsymbol{\mu}\boldsymbol{e}_k^T \frac{\partial \boldsymbol{h}(\hat{\boldsymbol{x}}_k)}{\partial \hat{\boldsymbol{x}}_k}. \tag{16}$$

From (16), we can see that when the error is zero, the expected value of the next state vector equals to that of the current state vector. As the error increases and/or the accumulated estimation bias increases, big jumps in the estimated state vectors should be expected. However, LMS is known for its stability even if large state-jumps occur, owing to the instantaneous gradient that constitutes the main component of its state-update formula.

An extended version of the LMS filter with smaller gradient noise is the normalized LMS (NLMS). With NLMS, we can change the step size according to the inverse of the $L2-$norm of $\hat{\boldsymbol{x}}_k$ as follows [26]:

$$\hat{\boldsymbol{x}}_{k+1} = \hat{\boldsymbol{x}}_k + \frac{2}{||\hat{\boldsymbol{x}}_k||_2} \boldsymbol{\mu}\boldsymbol{e}_k^T \frac{\partial \boldsymbol{h}(\hat{\boldsymbol{x}}_k)}{\partial \hat{\boldsymbol{x}}_k}. \tag{17}$$

B. The Recursive Least-Squares (RLS) Algorithm

Another powerful tracking method is the recursive least-squares (RLS) algorithm. In RLS, the dynamic state value at the current time instant is modeled as a weighted sum of the state values at the previous B time instances. B is usually called the RLS filter length. Clearly, the main embedded assumption here is that these B states are correlated. Since the tracked state is changing over time, correlation decreases over time and, thus, a forgetting factor, λ, is needed to give a higher importance weight to the most recent states as opposed to the distant states in time.

The role of the RLS filter is to adaptively track the complex weights, $\boldsymbol{w}_k \in \mathbb{C}^B$, each time a new measurement data is received using a scaled innovation vector, $\boldsymbol{e}_k$. The steps of the RLS algorithm can be stated as follows [26]:

1) Initialization: Given the initial weight vector $\hat{\boldsymbol{w}}_{0|0}$ and the initial weight covariance matrix $\boldsymbol{T}_{0|0} = \delta^{-1}\boldsymbol{I}$, where δ is a small positive constant.
2) Calculate the gain vector, $\boldsymbol{g}$:

$$\boldsymbol{g}_{k|k-1} = \frac{\lambda^{-1}\boldsymbol{T}_{k|k-1}\hat{\boldsymbol{x}}_{k|k-1}}{1 + \lambda^{-1}\hat{\boldsymbol{x}}_{k|k-1}^H \boldsymbol{T}_{k|k-1}\hat{\boldsymbol{x}}_{k|k-1}} \tag{18}$$

3) Calculate the current weight vector:

$$\hat{\boldsymbol{w}}_{k|k} = \hat{\boldsymbol{w}}_{k|k-1} + \boldsymbol{g}_{k|k-1}\Big(\boldsymbol{y}_k - \boldsymbol{h}(\hat{\boldsymbol{x}}_{k|k-1})\Big) \tag{19}$$

4) Calculate the current weight covariance matrix:

$$\boldsymbol{T}_{k|k} = \Big(\boldsymbol{I} - \boldsymbol{g}_{k|k-1}\boldsymbol{x}_{k|k-1}^{H}\Big)\lambda^{-1}\boldsymbol{T}_{k|k-1} \tag{20}$$

5) Estimate the current state vector:

$$\hat{\boldsymbol{x}}_{k|k} = \hat{\boldsymbol{w}}_{k|k}^{H}\hat{\boldsymbol{x}}_{k|k-1} \tag{21}$$

6) Repeat steps 2 to 5 until $\|\hat{\boldsymbol{x}}_{k|k-1} - \hat{\boldsymbol{x}}_{k|k}\|_2 \leq \Delta\boldsymbol{x}_{RLS}$, where $\Delta\boldsymbol{x}_{RLS}$ is a pre-set threshold constant, or until a desired number of iterations is reached. Note that this thresholding can also be performed for each state parameter in (5) separately as the quantities are different in nature (e.g. real angle values vs complex gain values).

The subscript $k|k-1$ should be read as "at time instant k given the measurements data at time instant $k-1$." RLS is known for its faster convergence relative to the LMS algorithm [28]. However, LMS is more capable of dealing with abrupt changes in the dynamics of the state, while with RLS these sudden changes may need to be detected and the algorithm should be re-started all over again to avoid tracking divergence, even though smooth re-initialization is also possible. Also, it is worth noting that the choice of the parameters of the step-size, $\boldsymbol{\mu}$, in LMS and the forgetting factor, λ, in RLS also affects the convergence and stability of these two algorithms [29]. In the actual implementation of the RLS algorithm, we used the extended RLS algorithm from [26].

C. The Extended Kalman Filter (EKF) Algorithm

Kalman filter (KF) is a state-space based framework for the estimation and tracking of a changing state of a dynamic system adaptively using innovation information. The main assumption in the basic form of the KF is that the model is linear and the noise is drawn from a unimodal Gaussian random process. For nonlinear systems (such as (8)), however, the extended Kalman filter (EKF) is usually used, where the system is linearized before the KF is applied, with a similar noise process assumption as in the standard KF. It is worth noting that if the noise variance is large and the state-space model is highly nonlinear, then the EKF with first-order linearization may not be guaranteed to converge. Thus, it is preferred to apply the EKF in moderate or high signal-to-noise ration (SNR) regions even for relatively highly nonlinear systems.

In this work, we apply the EKF to track the time-varying state-vector $\boldsymbol{x}$. Using the state-space model in (6) and (8), the sequential steps of the EKF algorithm (applied to our beam and channel tracking problem) are as follows [26]:

1) Initialization: Given the initial state vector $\hat{\boldsymbol{x}}_{0|0}$ and the initial state covariance matrix $\boldsymbol{P}_{0|0}$.
2) Calculate Kalman gain matrix, $\boldsymbol{G}$:

$$\boldsymbol{G}_{k|k-1} = \boldsymbol{P}_{k|k-1}\boldsymbol{H}_k^{H}\Big(\boldsymbol{H}_k\boldsymbol{P}_{k|k-1}\boldsymbol{H}_k^{H} + \boldsymbol{R}_k\Big)^{+} \tag{22}$$

3) Calculate the current state value:

$$\hat{\boldsymbol{X}}_{K|K} = \hat{\boldsymbol{X}}_{K|K-1} + \boldsymbol{G}_{K|K-1}\Big(\boldsymbol{Y}_K - \boldsymbol{H}(\hat{\boldsymbol{X}}_{K|K-1})\Big) \tag{23}$$

4) Calculate the current state covariance matrix:

$$\boldsymbol{P}_{k|k} = \Big(\boldsymbol{I} - \boldsymbol{G}_{k|k-1}\boldsymbol{H}_k\Big)\boldsymbol{P}_{k|k-1} \tag{24}$$

5) Predict the next state value:

$$\hat{\boldsymbol{x}}_{k+1|k} = \boldsymbol{F}_k\hat{\boldsymbol{x}}_{k|k} \tag{25}$$

6) Predict the next state covariance matrix (aka Riccati update equation):

$$\boldsymbol{P}_{k+1|k} = \boldsymbol{F}_k\boldsymbol{P}_{k|k}\boldsymbol{F}_k^{H} + \boldsymbol{Q}_k \tag{26}$$

7) Repeat steps 2 to 6 until $\|\hat{\boldsymbol{x}}_{k|k-1} - \hat{\boldsymbol{x}}_{k|k}\|_2 \leq \Delta\boldsymbol{x}_{EKF}$, where $\Delta\boldsymbol{x}_{EKF}$ is a pre-set threshold constant, or until a desired number of iterations is reached. Note that the thresholded state difference can also be done for each state value in (5) separately because the state members are different in nature (e.g. real angle values vs complex gain values).

The notation $(.)^{+}$ refers to the pseudo-inverse of the matrix $(.)$. The noise covaiance matrices are defined as: $\boldsymbol{R}_k = \mathbb{E}\{\boldsymbol{v}_k\boldsymbol{v}_k^{H}\}$ and $\boldsymbol{Q}_k = \mathbb{E}\{\boldsymbol{n}_k\boldsymbol{n}_k^{H}\}$. $\boldsymbol{I}$ is an identity matrix of a proper size.

The term inside the parentheses in (23) is the innovation vector and it shows the error between the actual received measurements at the current time instant and the predicted measurements from the model at the previous time instant. Since the measurements model in (8) is (highly) nonlinear in the state vector, large measurements-model mismatch may lead to tracking divergence, as we mentioned before. Also, depending on the velocity of the mobile receiver and the operation frequency, the coherence time should be long-enough to perform the tracking steps of the EKF, especially the pseudo-inverse operation in (22). Overall, as we will see in the results section, we can claim that the EKF tracker works best in situations where the channel is stationary or quasi-stationary, but may not be guaranteed to converge in nonstationary channels for the reasons mentioned earlier in this section.

IV. Simulation Results

In this section, we evaluate the overall performance of the LMS and RLS tracking filters, in addition to the celebrated extended Kalman filter (EKF), to serve two main objectives: 1) we compare these filters to, simultaneously track the DOA, DOD, and path gain in a single path ($L = 1$) and multipath ($L = 3$) environments, and 2) to emphasise the fact that evaluating these types of trackers based on individual state parameters rather than the overall system performance can lead to non-complete conclusions, such as those made in [9] and [11]. We use the MSE of the measurements (J, defined in §III-A), as well as the MSE of the DOA and DOD, as the evaluation metrics of our results.

To emphasise the role of the array aperture size, we consider two MIMO system scenarios with uniform linear array at both sides of the communication link: $M_R = M_T = 16$ and $M_R = M_T = 4$. Moreover, the pointing angles are taken as $\bar{\theta} = \bar{\phi} = 45^{\circ}$, and the noise variance of the DOA and DOD estimates is taken as $\sigma_{\theta}^2 = \sigma_{\phi}^2 = (0.5^{\circ})^2$. Moreover, the state correlation parameters $\rho_{\theta} = \rho_{\phi} = 1$ and $\rho_{\alpha} = 0.995$.

Based on an educated guess, we set the step-sizes of the LMS filter to $\mu_\theta = \mu_\phi = 10^{-6}$, and $\mu_\alpha = 10^{-3}$. In the RLS, the forgetting factor is chosen to be $\lambda = 0.995$. Two scenarios are considered in our simulations: the single path case, $L = 1$, (i.e. line-of-sight path, LoS), and the multipath case, where the information is communicated over $L = 3$ dominant paths sharing the same mean value (the pointing angle). The rational behind the later case is that, usually, in mmWave wireless communication systems the receiver expects a single dominant LoS path to be received, even though more random paths can dominate the communication link, which can happen, for example, when a reflector is placed close to the receiver or the transmitter. The SNR of the main path is 30 dB, while the multipath components have 3dB SNR.

It is worth noting that the curves presented in this section may change if the initial states change. However, this mainly depends on the antenna array beamwidth, where wide beams are more tolerant to initial values than narrow beams. Also, as long as the initial values of the DOA and DOD angles are within the 3dB beamwidth of each other, the tracker can always recover.

Figs. 1 and 2 show the MSE performance of the LMS, RLS, and EKF for the case of $M_R = M_T = 16$ antenna elements. Even though the LMS and RLS have similar performance in the angular domain, the overall system performance is different, and the EKF stands out as the best among the three trackers. The reason for this behavior is that the MSE of the innovation process captures the relationship among DOA, DOD, and channel gain simultaneously, which gives a better system-level understanding about the performance of these trackers. Also, the transmit-receive beams mismatch increases over time since the estimation error accumulates and propagates through the states, as can be projected from the system model and the state-space model.

Reducing the number of antenna elements leads to a lower beamforming gain, but at the same tiem the quality of the tracking improves, as shown in Figs. 3 and 4. In addition, since the ratio of the array beamwidth to the state noise variance of the DOA and DOD decreases as we add more antennas (i.e. the beam becomes narrower), the trackers become more sensitive to small tracking errors and small variations in the angular location of the target user. It is for this reason that the curves in Figs. 3 and 4 are smoother than those in Figs. 1 and 2 and the MSE is smaller too. Also, since the user location is assumed to vary slowly and smoothly in our simulations, and since there is no abrupt changes in the channel link, the curves of the LMS and RLS algorithms are very close.

In Fig. 5, we plot the MSE of the innovation in single path ($L = 1$) and multipath ($L = 3$) environments using LMS, RLS, and EKF algorithms for $M_T = M_R = 16$ antenna elements. We can notice that the MSE increases substantially in the case of multipath. The reason for this performance degradation from $L = 1$ to $L = 3$ paths is that the tracker's model assumes a single path and did not account for the other two (weaker) paths, which can be seen as two weak sources of interference. Also, the three used algorithms behave similarly in the single path and multipath scenarios. Thus, it is recommended that the tracker is capable of tracking more than a single dominant path to avoid occasional beam misalignment or loss of connectivity. In addition, the tracker must be reset (or re-initialized) when the MSE of the DOA hits a specific threshold to avoid tracking divergence.

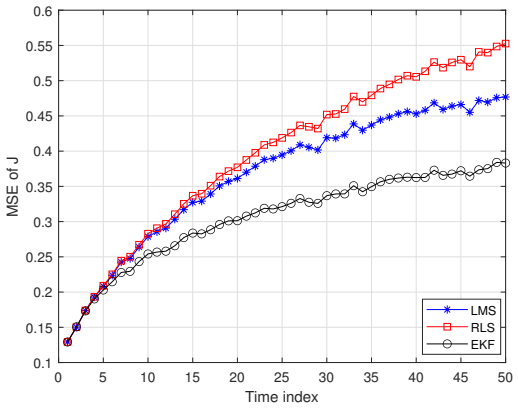

Fig. 1. Overall MSE of LMS, RLS, and EKF for $M_R = M_T = 16$ antenna elements with $L = 1$ path.

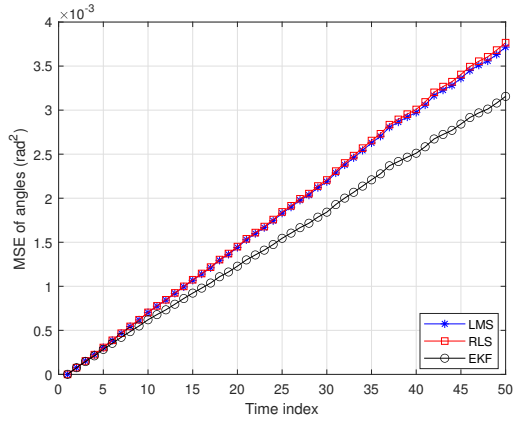

Fig. 2. MSE of the DOA of LMS, RLS, and EKF for $M_R = M_T = 16$ antenna elements with $L = 1$ path.

In mmWave systems, the array size could be different at the communication sides. The behavior of the MSE curves presented in this section for the case of equal number of antennas at the TX and RX sides is not different from the case of unequal number of antennas at both sides. However, the results can improve since the beamwidth at one side will be wider than the other side, which improves the tracking quality at the expense of smaller communication rate due to the reduction in the array gain.

V. Conclusion

In this paper, the LMS, RLS, and EKF tracking filters are used to track the DOA, DOD, and channel gain in single and multipath environments. We use the MSE of the innovation random process, in addition to the MSE of the DOA and DOD, as our evaluation metric to assess these three filters. We showed that if the communication link contains more than a single dominant path, a large MSE performance degradation is observed, unless the tracking filter is designed to handle

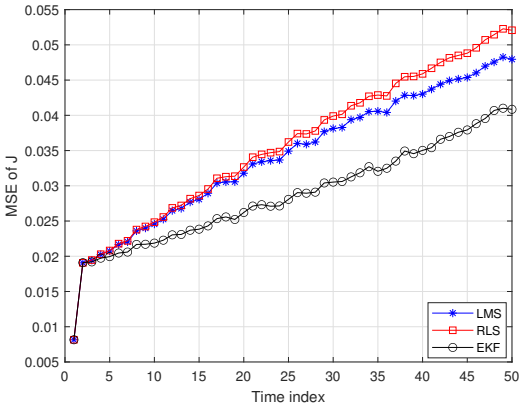

Fig. 3. Overall MSE of LMS, RLS, and EKF for $M_R = M_T = 4$ antenna elements with $L = 1$ path.

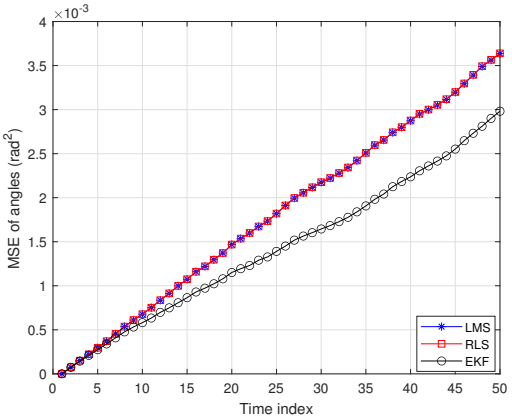

Fig. 4. MSE of the DOA of LMS, RLS, and EKF for $M_R = M_T = 4$ antenna elements with $L = 1$ path.

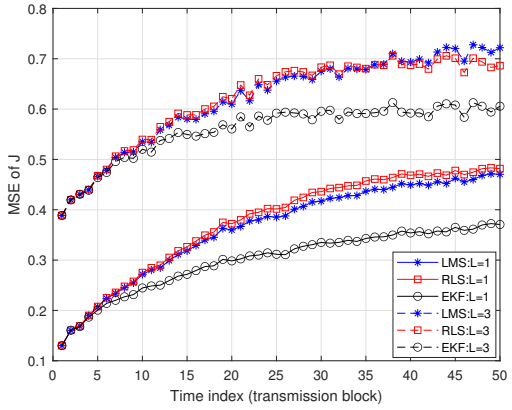

Fig. 5. Overall MSE performance comparison between LMS, RLS, and EKF for $M_R = M_T = 16$ antenna elements with LOS ($L = 1$) and multipath environments ($L = 3$).

variable number of paths. Moreover, we observed that investigating the individual state variables can lead to an incomplete conclusion. The MSE of the innovation process captures the overall system performance rather than the individual channel and beam parameters. Also, we noticed that LMS and RLS trackers have similar MSE performance in beam tracking applications, while the EKF stands out due to its ability to capture correlation information of the measurements and the state.

REFERENCES

[1] S. A. Busari, K. M. S. Huq, S. Mumtaz, L. Dai, and J. Rodriguez, "Millimeter-wave massive mimo communication for future wireless systems: A survey," *IEEE Communications Surveys & Tutorials*, vol. 20, no. 2, pp. 836–869, 2017.

[2] W. A. Awan, N. Hussain, A. Ghaffar, A. Zaidi, S. I. Naqvi, and X. J. Li, "Compact flexible frequency reconfigurable antenna for heterogeneous applications," in *2020 9th Asia-Pacific Conference on Antennas and Propagation (APCAP)*. IEEE, 2020, pp. 1–2.

[3] W. A. Awan, N. Hussain, S. A. Naqvi, A. Iqbal, R. Striker, D. Mitra, and B. D. Braaten, "A miniaturized wideband and multi-band on-demand reconfigurable antenna for compact and portable devices," *AEU-International Journal of Electronics and Communications*, vol. 122, p. 153266, 2020.

[4] A. Ghaffar, W. A. Awan, N. Hussain, S. Ahmad, and X. J. Li, "A compact dual-band flexible antenna for applications at 900 and 2450 mhz," *Progress In Electromagnetics Research Letters*, vol. 99, no. 00, pp. 83–92, 2021.

[5] H. Shokri-Ghadikolaei and C. Fischione, "The transitional behavior of interference in millimeter wave networks and its impact on medium access control," *IEEE Transactions on Communications*, vol. 64, no. 2, pp. 723–740, 2016.

[6] M. Cheng, J.-B. Wang, Y. Wu, X.-G. Xia, K.-K. Wong, and M. Lin, "Coverage analysis for millimeter wave cellular networks with imperfect beam alignment," *IEEE Transactions on Vehicular Technology*, vol. 67, no. 9, pp. 8302–8314, 2018.

[7] M. Comisso and F. Babich, "Coverage analysis for 2d/3d millimeter wave peer-to-peer networks," *IEEE Transactions on Wireless Communications*, vol. 18, no. 7, pp. 3613–3627, 2019.

[8] A. M. Sayeed, "Deconstructing multiantenna fading channels," *IEEE Transactions on Signal processing*, vol. 50, no. 10, pp. 2563–2579, 2002.

[9] V. Va, H. Vikalo, and R. W. Heath, "Beam tracking for mobile millimeter wave communication systems," in *2016 IEEE Global Conference on Signal and Information Processing (GlobalSIP)*. IEEE, 2016, pp. 743–747.

[10] S. Shaham, M. Kokshoorn, M. Ding, Z. Lin, and M. Shirvanimoghaddam, "Extended kalman filter beam tracking for millimeter wave vehicular communications," in *2020 IEEE International Conference on Communications Workshops (ICC Workshops)*. IEEE, 2020, pp. 1–6.

[11] Y. Yapıcı and I. Güvenç, "Low-complexity adaptive beam and channel tracking for mobile mmwave communications," in *2018 52nd Asilomar Conference on Signals, Systems, and Computers*. IEEE, 2018, pp. 572–576.

[12] H. Chung, J. Kang, H. Kim, Y. M. Park, and S. Kim, "Adaptive beamwidth control for mmwave beam tracking," *IEEE Communications Letters*, vol. 25, no. 1, pp. 137–141, 2020.

[13] C. Zhang, D. Guo, and P. Fan, "Tracking angles of departure and arrival in a mobile millimeter wave channel," in *2016 IEEE International Conference on Communications (ICC)*. IEEE, 2016, pp. 1–6.

[14] S. Shaham, M. Ding, M. Kokshoorn, Z. Lin, S. Dang, and R. Abbas, "Fast channel estimation and beam tracking for millimeter wave vehicular communications," *IEEE Access*, vol. 7, pp. 141 104–141 118, 2019.

[15] J. Kang, I. Orikumhi, Y.-M. Park, and S. Kim, "A millimeter wave beam tracking in vehicular scenario via particle filter," in *2018 International Conference on Network Infrastructure and Digital Content (IC-NIDC)*. IEEE, 2018, pp. 234–238.

[16] S. Blandino, T. Bertrand, C. Desset, A. Bourdoux, S. Pollin, and J. Louveaux, "A blind beam tracking scheme for millimeter wave systems," in *2020 IEEE 91st Vehicular Technology Conference (VTC2020-Spring)*. IEEE, 2020, pp. 1–6.

[17] S. H. Lim, S. Kim, B. Shim, and J. W. Choi, "Deep learning-based beam tracking for millimeter-wave communications under mobility," *arXiv preprint arXiv:2102.09785*, 2021.

[18] D. Burghal, N. A. Abbasi, and A. F. Molisch, "A machine learning solution for beam tracking in mmwave systems," in *2019 53rd Asilomar Conference on Signals, Systems, and Computers*. IEEE, 2019, pp. 173–177.
[19] I. Panda and S. Ramanath, "Learning based beam tracking in 5g nr," in *2020 International Conference on COMmunication Systems & NETworkS (COMSNETS)*. IEEE, 2020, pp. 646–649.
[20] M. Shinzaki, Y. Koda, K. Yamamoto, T. Nishio, M. Morikura, C.-h. Huang, Y. Shirato, and N. Kita, "Deep reinforcement learning-based beam tracking from mmwave antennas installed on overhead messenger wires," in *2020 IEEE 92nd Vehicular Technology Conference (VTC2020-Fall)*. IEEE, 2020, pp. 1–6.
[21] E. Björnson, H. Wymeersch, B. Matthiesen, P. Popovski, L. Sanguinetti, and E. de Carvalho, "Reconfigurable intelligent surfaces: A signal processing perspective with wireless applications," *arXiv preprint arXiv:2102.00742*, 2021.
[22] M. R. Akdeniz, Y. Liu, M. K. Samimi, S. Sun, S. Rangan, T. S. Rappaport, and E. Erkip, "Millimeter wave channel modeling and cellular capacity evaluation," *IEEE journal on selected areas in communications*, vol. 32, no. 6, pp. 1164–1179, 2014.
[23] R. W. Heath, N. Gonzalez-Prelcic, S. Rangan, W. Roh, and A. M. Sayeed, "An overview of signal processing techniques for millimeter wave mimo systems," *IEEE journal of selected topics in signal processing*, vol. 10, no. 3, pp. 436–453, 2016.
[24] M. Arnold, X. Milner, H. Witte, R. Bauer, and C. Braun, "Adaptive ar modeling of nonstationary time series by means of kalman filtering," *IEEE transactions on biomedical engineering*, vol. 45, no. 5, pp. 553–562, 1998.
[25] S. Jayaprakasam, X. Ma, J. W. Choi, and S. Kim, "Robust beam-tracking for mmwave mobile communications," *IEEE Communications Letters*, vol. 21, no. 12, pp. 2654–2657, 2017.
[26] S. Haykin, *Adaptive filter theory*, 5th ed. Pearson, 2014.
[27] H. L. Van Trees, *Optimum array processing*. New York: Wiley, 2002.
[28] E. Eweda and O. Macchi, "Convergence of the RLS and LMS adaptive filters," *IEEE Transactions on Circuits and Systems*, vol. 34, no. 7, pp. 799–803, 1987.
[29] E. Eleftheriou and D. Falconer, "Tracking properties and steady-state performance of RLS adaptive filter algorithms," *IEEE transactions on acoustics, speech, and signal processing*, vol. 34, no. 5, pp. 1097–1110, 1986.

Mohanad Al-Ibadi received the B.Sc. and M.Sc. degrees in electrical engineering from the University of Technology in Baghdad, Baghdad, Iraq, in 2006 and 2009, respectively, and the Ph.D. degree in electrical engineering from the University of Kansas, Lawrence, KS, USA, in 2019. He is currently a Faculty Member with the Engineering Technical College of Najaf at Al-Furat Al-Awsat Technical University, Iraq. Formerly, he was a Graduate Research Assistant with the Center for Remote Sensing of Ice-Sheets (CReSIS). His current research interests include the area of array signal processing for radar and wireless communications, in addition to energy optimization in wireless sensor networks.

Farhad E. Mahmood received the B.S., and M.S. degrees from the University of Mosul, in 2005, and 2008, respectively, and received the Ph.D. degree from The University of Kansas, the USA in 2019, all in electrical engineering University of Mosul. His research interests include wireless communications, energy efficiency, Machine learning, and signal processing. Dr. Mahmood is a reviewer in several IEEE Transaction journals.